

Deletion of inducible nitric oxide synthase delays the onset of cardiomyocyte electrical remodeling in experimental Chagas disease

Danilo Roman-Campos^{a,*}, Policarpo Sales-Junior^c, Artur Santos-Miranda^a, Julliane V. Joviano-Santos^a, Catherine Ropert^b, Jader S. Cruz^{b,**}

^a Laboratory of CardioBiology, Department of Biophysics, Universidade Federal de São Paulo, São Paulo, Brazil

^b Department of Biochemistry and Immunology, Biological Sciences Institute, Universidade Federal de Minas Gerais, Brazil

^c René Rachou Institute, Oswaldo Cruz Foundation, Minas Gerais, Brazil

Chagas disease (CD), caused by the protozoan parasite *Trypanosoma cruzi*, has become a global health problem due to the massive migration flow from Latin America to other parts of the globe, including Europe [1,2]. The disease is the most common infective cause of cardiomyopathy and it is observed in 11–19% of patients in Europe [3]. The time course of the disease is complex and 20–30% of patients with 10–30 years after infection will develop heart failure and/or arrhythmias. Despite its importance, there is scarce information about the molecular physiopathology of the heart in CD. It is known that inducible nitric oxide synthase (iNOS) plays an important role in the macrophage-driven control of parasitic infection, through the formation of peroxynitrite [4–6]. However, nitric oxide (NO) is an important modulator of cell machinery and its unbalanced production aggravates electrical disturbances during experimental CD [7–10]. We hypothesized that activation of iNOS plays an important role on the electrical remodeling of cardiomyocytes in the acute phase of experimental CD. Thus, we evaluated if iNOS takes part in electrical remodeling of isolated cardiomyocyte in the time course of the acute phase of experimental CD.

Eight-week-old male/female C57BL/6 and iNOS^{-/-} mice were infected intraperitoneally with 50 bloodstream trypomastigote form of colombian strain of *T. cruzi*. Mouse Inflammation Kit from BDTM was used to detect serum cytokine levels. The animals were kindly provided by Professor Dr. Ricardo T. Gazzinelli.

Left ventricular cardiomyocytes were obtained using an enzymatic dissociation method with collagenase type II, as previously described [11–13]. Only calcium-tolerant, quiescent, rod-shaped myocytes showing clear cross striations were studied. Isolated cardiomyocytes from non-infected and infected mice were studied at 15 and 30 days post-infection (dpi).

Patch-clamp recordings were obtained using an EPC-9.2 patch-clamp amplifier. To measure action potentials (AP) and outward K⁺

currents (I_K) the pipette solution had (in mM): 130 K-aspartate, 20 KCl, 10 HEPES, 2 MgCl₂, 5 NaCl, 5 EGTA, pH set to 7.2 with KOH. We used Tyrode's as bath solution (in mM) 140 NaCl, 5.4 KCl, 1 MgCl₂, 1.8 CaCl₂, 10 HEPES, 10 glucose (pH set at 7.4). To record total outward I_K cardiac myocytes were bathed with recording solution containing 100 μM of Cd²⁺ to block L-type Ca²⁺ currents. Total I_K was measured by depolarization steps from -40 to 50 mV (3 s duration) from a holding potential of -80 mV every 15 s. For measurements of L type Ca²⁺ current (I_{CaL}), recording pipettes were filled with internal solution containing (in mM): 120 CsCl, 20 TEACL, 5 NaCl, 10 HEPES, 5 EGTA, pH set to 7.2 with CsOH. I_{CaL} was measured using 1.8 mM of Ca²⁺ in extracellular solution. Membrane potential was first stepped from a holding potential of -80 mV to -40 mV for 50 ms and then stepped to different membrane voltages from -40 to 50 mV (300 ms duration). Junction potential was not corrected. The complete patch-clamp methodology is described in [12].

Data are expressed as mean ± standard error (SE) and the number of samples is shown as n. Statistical significance of parametric data between multiple groups was determined by one-way or two-way ANOVA, followed by Tukey's post-test. For patch-clamp experiments cardiomyocytes were obtained from at least three animals for each measurement. Survival rate was analyzed using Kaplan-Meier plot. Comparisons were considered to be statistically significant when $p < 0.05$. During the acute phase of experimental CD excessive NO production contributes to the impairment of electrical properties in cardiomyocytes [12]. Thus, we hypothesized that the deletion of iNOS, which is highly activated through IFN-γ activation pathway during the course of the disease, would attenuate the electrical remodeling of cardiomyocytes. Parasitemia were similar for both groups at 15 dpi. However, it was higher in iNOS^{-/-} mice at 30 dpi (Fig. 1A). Higher parasitism was associated with increased, yet not significant, mortality rate in knockout (KO) mice (Fig. 1B) between 20 and 40 dpi, however,

* Correspondence to: D. Roman-Campos, Laboratory of CardioBiology, 2 Andar, Edifício de Ciências Biomédicas, Universidade Federal de São Paulo, Rua Botucatu 862, Vila Clementino, São Paulo, São Paulo 04023062, Brazil.

** Correspondence to: J.S. Cruz, Laboratório de Membranas Excitáveis e de Biologia Cardiovascular, Departamento de Bioquímica e Imunologia, Bloco H4, Sala 480, Av Antonio Carlos, 6627, Pampulha, Belo Horizonte, Minas Gerais 3016970, Brazil.

E-mail addresses: drcampos@unifesp.br (D. Roman-Campos), jacruz@ufmg.br (J.S. Cruz).

<https://doi.org/10.1016/j.bbadis.2020.165949>

Received 3 July 2020; Received in revised form 17 August 2020; Accepted 19 August 2020

Available online 22 August 2020

0925-4439/ © 2020 Elsevier B.V. All rights reserved.

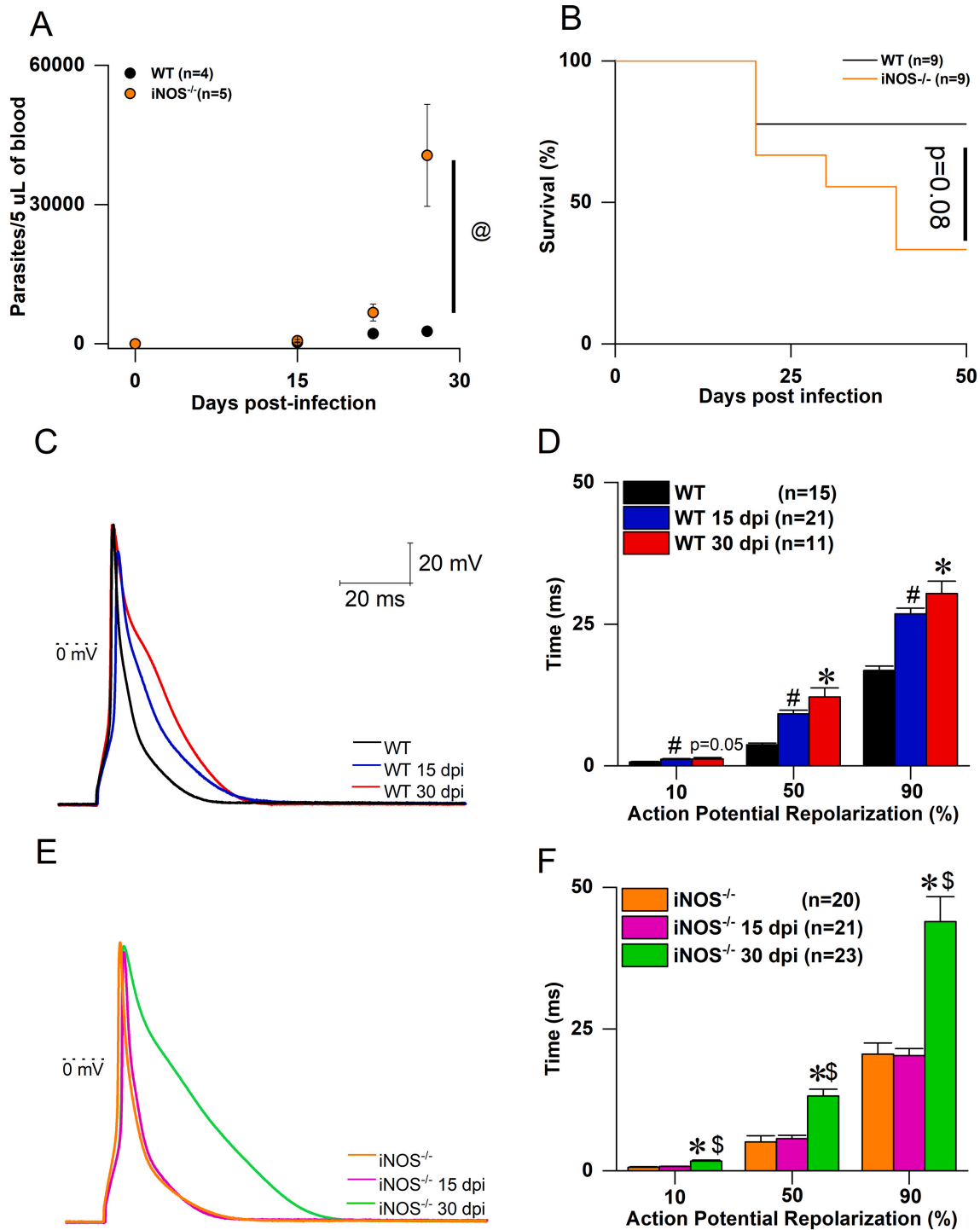


Fig. 1. (A) Parasitemia curves were taken from WT (n = 5) and iNOS (n = 5) mice. (B) Mortality curves were created using 9 animals/group. (C) Representative superimposed action potentials measured in WT (black line), WT 15 days post-infection (dpi) (blue line) and 30 dpi (red line). (D) Time to action potential repolarization at different repolarization levels in non-infected, 15 dpi and 30 dpi mice. (E) Representative superimposed action potentials measured in iNOS^{-/-} (orange line), iNOS^{-/-} 15 dpi (magenta line) and 30 dpi (green line). Scale bar is the same for (C) and (E). (F) Time required to reach 10%, 50% and 90% of action potential repolarization in non-infected, 15 dpi and 30 dpi iNOS^{-/-} mice. **p* < 0.05. Mortality curves were analyzed using Kaplan-Meier estimator; Two-way ANOVA for analysis of parasite levels @ comparing WT and iNOS^{-/-} mice; one-way ANOVA for analysis of action potential repolarization (*before infection versus 30 dpi, # before infection versus 15 dpi; \$ 15 versus 30 dpi).

at initial stages of the disease (15 dpi) no mice died in both groups. Additionally, both infected groups had the same serum levels of IFN γ , MCP-1, IL-10, IL-6, IL-12p70, and TNF at 15 dpi (*p* > 0.05, n = 3/each group, data not shown). Fig. 1C and E show representative superimposed traces of AP measured in WT and iNOS^{-/-} before infection and at 15 and 30 dpi, respectively. It is clear that infection caused

lengthening of AP duration in cardiomyocytes at 15 dpi in WT which was still observed at 30 dpi. However, iNOS^{-/-} at 15 dpi did not show significant changes in AP duration, although at 30 dpi AP duration was increased. Summarized data for AP duration at 10, 50, and 90% of repolarization is shown in Fig. 1D and F.

The proper control of AP waveform in cardiomyocytes is the result

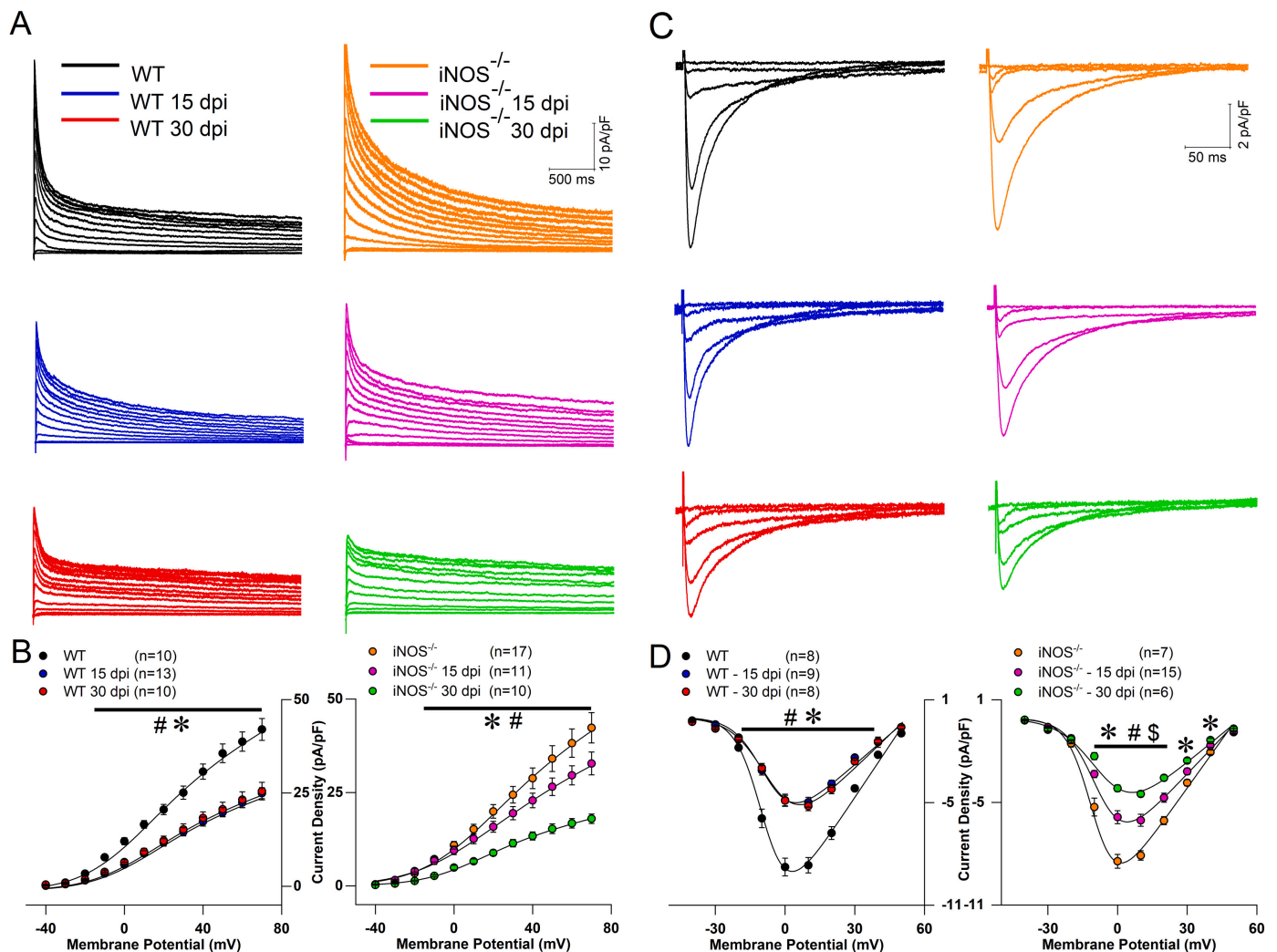


Fig. 2. (A) Representative outward potassium current (I_K) traces for WT (left) and $iNOS^{-/-}$ (right) at zero, 15 and 30 days post-infection (dpi). Scale bar for I_K is equal for all traces. (B) Current density-voltage relationships for tested membrane potentials. (C) Representative calcium current (I_{CaL}) traces for WT (left) and $iNOS^{-/-}$ mice (right) non-infected and 15 and 30 dpi. Scale bar for I_{CaL} is equal for all traces. (D) Current density-voltage relationships for tested membrane potentials. Continuous lines (B) and (D) are the best fit using the Boltzmann function. $p < 0.05$ using one-way ANOVA. (* before infection versus 30 dpi, # before infection versus 15 dpi; \$ 15 versus 30 dpi).

of steady-state ion currents found in the sarcolemma, with major contributors of I_K and I_{CaL} . Thus, we decided to investigate if changes in these currents could explain the observed phenotype in the AP waveform. As shown in Fig. 2A and C, which are representative traces of I_K and I_{CaL} , *T. cruzi* infection led to a significant attenuation of both currents at 15 and 30 dpi from WT mice. However, when these currents were studied in cardiomyocytes from $iNOS^{-/-}$ it is evident that I_K was not attenuated and reduction of I_{CaL} was not as severe as for WT at 15 dpi. Nonetheless, both groups showed similar results in studied cardiomyocytes at 30 dpi. Composite data for tested membrane potentials are show in Fig. 2B (I_K) and Fig. 2D (I_{CaL}).

In this study, we showed that *T. cruzi* infection: (i) induced higher parasite levels that correlated with an increase mortality rate in $iNOS^{-/-}$ mice; (ii) caused marked AP prolongation and reduced I_K and I_{CaL} current densities in cardiomyocytes from WT and $iNOS^{-/-}$ mice; and (iii) the electrical remodeling was attenuated in cardiomyocytes from $iNOS^{-/-}$ mice at 15 dpi and reached WT levels at 30 dpi. In the acute phase, macrophages-dependent production of NO plays a beneficial role as a trypanocidal agent through the IFN- γ -iNOS axis [5]. Conversely, NO overproduction via iNOS/NOS2 activity has been implicated in heart injury in *T. cruzi*-infected monkeys and mice (4–7). In this regard, excessive iNOS expression has long been associated with worst

prognostic of heart failure in humans [14]. However, despite major importance of iNOS for the outcome of CD there was no information on its role in the electrical remodeling of cardiomyocytes in CD.

The main observation of this study is that early in the acute phase the absence of iNOS and consequently iNOS-dependent NO (iNO) production does not interfere with parasite burn or mice mortality but prevented cardiomyocytes electrical remodeling. Cytokine levels were similar in WT and $iNOS^{-/-}$ mice at this stage. This allowed us to conclude that NO plays a stage-dependent role, becoming protective against parasite proliferation but only late in the acute infection. This is in accordance with previous reports of NO as an important mediator produced by phagocytes that constitute the first line of microbial defense, sensing the presence of different types of infectious agents [15]. This explain the differences in parasitemia curve observed between both groups.

In a previous study from our group, we reported that NO was a significant determinant of I_{CaL} remodeling in cardiomyocytes from WT at 30 dpi. Importantly, iNOS deletion did not prevent the reduction of I_{CaL} [12], which was confirmed in our present study since $iNOS^{-/-}$ displayed attenuation of I_{CaL} at 30 dpi. However, it is still not clear if remodeling of cardiomyocytes at 30 dpi is dependent on the increased parasitemia and possibly heart parasitism in $iNOS^{-/-}$ mice.

Furthermore, cardiomyocytes also have the presence of constitutive isoforms of nitric oxidase synthase, the neuronal (nNOS) and endothelial (eNOS). Importantly, both of them have a major role in the control of excitability in cardiomyocytes [16]. Thus, we may not disregard the participation of nNOS and eNOS in the electrical remodeling of cardiomyocytes in our experimental animal model. Additional studies are necessary to uncover these aspects. Nevertheless, evidence provided in our present study indicates that at in early stages of experimental CD, iNOS plays an important role in the electrical remodeling of cardiomyocytes. Selectively targeting it, in the heart tissue, might delay the onset of electrical remodeling during *T. cruzi* infection, while still controlling parasite burn.

Funding

This work was supported by São Paulo Research Foundation (FAPESP Grants # 2014/09861-1 and # 2019/21304-4 to DRC). A. Santos-Miranda holds a fellowship from São Paulo Research Foundation (FAPESP # 2018/22830-9). J.V. Joviano-Santos holds a fellowship from São Paulo Research Foundation (FAPESP #2018/20777-3). Fundação de Amparo à Pesquisa do Estado de Minas Gerais (FAPEMIG - PRONEX to JSC). CNPq - Conselho Nacional de Desenvolvimento Científico e Tecnológico (J.S.C. Grant #312474/2017-2). Funding source(s) had no involvement in study design; in the collection, analysis and interpretation of data; then this should be stated.

ORCID iD authorship contribution statement

Danilo Roman-Campos: Conceptualization, Data curation, Formal analysis, Funding acquisition, Investigation, Methodology, Writing - original draft, Writing - review & editing. **Policarpo Sales-Junior:** Formal analysis, Investigation. **Artur Santos-Miranda:** Formal analysis, Writing - original draft, Writing - review & editing. **Julliane V. Joviano-Santos:** Formal analysis, Writing - original draft, Writing - review & editing. **Catherine Ropert:** Investigation, Methodology, Writing - original draft, Writing - review & editing. **Jader S. Cruz:** Conceptualization, Funding acquisition, Supervision, Writing - original draft, Writing - review & editing.

Declaration of competing interest

The authors declare that they have no known competing financial interests or personal relationships that could have appeared to influence the work reported in this paper.

References

- [1] WHO, Fact Sheets—Chagas Disease, World Health Organization, 2020, p. 1.
- [2] K.C.F. Lidani, et al., Chagas disease: from discovery to a worldwide health problem, *Front. Public Health* 7 (2019) 166.
- [3] S. Antinori, et al., Chagas disease in Europe: a review for the internist in the globalized world, *Eur. J. Intern. Med.* 43 (2017) 6–15.
- [4] M.N. Alvarez, et al., Intraphagosomal peroxynitrite as a macrophage-derived cytotoxin against internalized *Trypanosoma cruzi*: consequences for oxidative killing and role of microbial peroxiredoxins in infectivity, *J. Biol. Chem.* 286 (8) (2011) 6627–6640.
- [5] R.T. Gazzinelli, et al., The microbicidal activity of interferon-gamma-treated macrophages against *Trypanosoma cruzi* involves an L-arginine-dependent, nitrogen oxide-mediated mechanism inhibitable by interleukin-10 and transforming growth factor-beta, *Eur. J. Immunol.* 22 (10) (1992) 2501–2506.
- [6] L. Piacenza, et al., Fighting the oxidative assault: the *Trypanosoma cruzi* journey to infection, *Curr. Opin. Microbiol.* 12 (4) (2009) 415–421.
- [7] C.M. Carvalho, et al., Inducible nitric oxide synthase in heart tissue and nitric oxide in serum of *Trypanosoma cruzi*-infected rhesus monkeys: association with heart injury, *PLoS Negl. Trop. Dis.* 6 (5) (2012) e1644.
- [8] M. Chandra, et al., Significance of inducible nitric oxide synthase in acute myocarditis caused by *Trypanosoma cruzi* (Tulahuen strain), *Int. J. Parasitol.* 32 (7) (2002) 897–905.
- [9] H. Huang, et al., Expression of cardiac cytokines and inducible form of nitric oxide synthase (NOS2) in *Trypanosoma cruzi*-infected mice, *J. Mol. Cell. Cardiol.* 31 (1) (1999) 75–88.
- [10] S. Carbajosa, et al., L-arginine supplementation reduces mortality and improves disease outcome in mice infected with *Trypanosoma cruzi*, *PLoS Negl. Trop. Dis.* 12 (1) (2018) e0006179.
- [11] A. Santos-Miranda, et al., Reactive oxygen species and nitric oxide imbalances lead to in vivo and in vitro arrhythmic phenotype in acute phase of experimental Chagas disease, *PLoS Pathog.* 16 (3) (2020) e1008379.
- [12] D. Roman-Campos, et al., Novel insights into the development of chagasic cardiomyopathy: role of PI3Kinase/NO axis, *Int. J. Cardiol.* 167 (6) (2013) 3011–3020.
- [13] D. Roman-Campos, et al., Changes in cellular contractility and cytokines profile during *Trypanosoma cruzi* infection in mice, *Basic Res. Cardiol.* 104 (3) (2009) 238–246.
- [14] G.A. Haywood, et al., Expression of inducible nitric oxide synthase in human heart failure, *Circulation* 93 (6) (1996) 1087–1094.
- [15] M. Carneiro-Sampaio, A. Coutinho, Tolerance and autoimmunity: lessons at the bedside of primary immunodeficiencies, *Adv. Immunol.* 95 (2007) 51–82.
- [16] M. Seddon, A.M. Shah, B. Casadei, Cardiomyocytes as effectors of nitric oxide signalling, *Cardiovasc. Res.* 75 (2) (2007) 315–326.